

Enhanced Reach of a Rod Injected into a Cylindrical Constraint by On-Off
Injection and Rotation

by

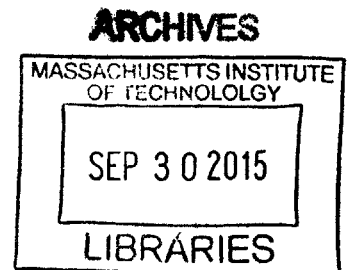
Ryan A. McDermott

Submitted to the
Department of Mechanical Engineering
in Partial Fulfillment of the Requirements for the Degree of
Bachelor of Science in Mechanical Engineering

at the

Massachusetts Institute of Technology

June 2015



© 2015 Ryan A. McDermott. All rights reserved.

The author hereby grants to MIT permission to reproduce and to distribute
publicly paper and electronic copies of this thesis document in whole
or in part in any medium now known or hereafter created

Signature of Author: Signature redacted
Department of Mechanical Engineering
May 18, 2015

Certified by: Signature redacted
Pedro M. Reis
Assistant Professor of Mechanical Engineering and Civil & Environmental Engineering
Thesis Supervisor

Accepted by: Signature redacted
Anette Hosoi
Professor of Mechanical Engineering
Undergraduate Officer

Enhanced Reach of a Rod Injected into a Cylindrical Constraint by On-Off Injection and Rotation

by

Ryan McDermott

Submitted to the Department of Mechanical Engineering on
May 18, 2015 in Partial Fulfillment of the Requirements for the
Degree of Bachelor of Science in Mechanical Engineering

Abstract

Using a desktop scale analog for the injection of a thin rod into a horizontal pipe to service wellbores in the oil industry, we perform an experimental investigation of the effect of rotating a thin rod as it undergoes on-off injection into a cylindrical constraint. When a thin rod is injected into a cylindrical constraint, the force required to continue injection increases over time, thus causing stresses to build inside the rod. These stresses eventually lead to buckling configurations, which can be described as sinusoidal and helical. If the stress in the rod continues to increase while in a helical configuration, the rod will reach a “lock-up” state, where the rod can no longer progress through the cylinder. To perform experiments, a custom manufactured elastic rod is injected into a borosilicate tube. A rotating apparatus was designed and constructed to rotate the rod at the injection site, allowing rotation to propagate through the entire rod, thus causing the length until lock-up to increase. This enhanced reach is directly proportional to rotation speed and radius of the rod, and inversely proportional to injection speed. Initial experiments examined the effect of rotation speed on the release time, which is the time required for a rod in a helical configuration to release into a straight configuration while experiencing rotation. The relationship between rotation speed and release time is exponential, with slower rotation speeds having a large release time and faster rotation speeds reaching an asymptote. The relationship between helical initiation length and release time is linear, but release times vary significantly for the same helical initiation lengths. On-off injection consisted of using a stepper motor to inject the rod with a square wave function that had a 50% duty cycle. The lock up length and helical initiation length were examined for different square wave periods. On-off injection with rotation can enhance the rod’s reach by at least 175% as compared to the only rotation condition. This is evidence that on-off injection can significantly enhance the reach of rods injected into cylindrical constraints.

Thesis Supervisor: Pedro Reis

Title: Assistant Professor of Mechanical Engineering and Civil & Environmental Engineering

Acknowledgments

I would like to thank my supervisor, Professor Pedro Reis, for all of his support over the past two years. Being a part of EGS Lab has helped me learn more than I ever expected, and I could not be more thankful for having Professor Reis as an adviser.

In addition, I would like to thank Connor Mulcahy for his advice and expertise in all areas related to this project. I would also like to thank Halla Moore for all her assistance with my writing and editing process.

Contents:

1	Introduction	8
1.1	Motivation	8
1.2	Previous Work	9
1.2.1	Compression of a Rod inside a Cylinder	9
1.2.2	Static Injection	10
1.3	Rotation Injection Theory	13
1.3.1	Rotation Injection Experiments	15
1.4	Rotation with On-Off Injection	17
2	Experiment	18
2.1	Experiment Apparatus Design	18
2.1.1	Injection Platform.	19
2.1.2	Rotating Assembly	20
2.1.3	Rod Storage	22
2.1.4	Borosilicate Tubing	23
2.1.5	AC Servo Motor and Electronics.	24
2.2	Experiment Preparation	25
2.2.1	Rod Cleaning Process	26
2.2.2	Tube Cleaning Process	26
2.3	Data Acquisition	27
2.3.1	Release Time Experimentation	27
2.3.2	On-Off Injection Experimentation	29
2.3.3	Video Recording and Analysis	30
3	Analysis and Results	32
3.1	Release Time	32
3.1.1	Dependence of the Release Time on the Rotation Speed.	33
3.1.2	Dependence of the Release Time on Helical Buckling Length	36
3.2	On-Off Injection	37
4	Conclusion	40

List of Figures

1.1	a.) Rod in a straight configuration b.) Rod in sinusoidal configuration c.) Rod in helical configuration	9
1.2	Helix initiation length compared to radian clearance. Radian clearance is depicted in the bottom left of plot. Figure adapted from [10].	12
1.3	Axial view of the rod inside a cylinder. Gravitation force pushes down, but normal force is at an angle relative to the vertical axis.	13
1.4	Top view of the forces acting upon the rod as it moves through the cylindrical constraint. Figure adapted from [13]	14
1.5	Normalized injection length for parameter α . Data collected for different radial clearances. Figure adapted from [13].	16
1.6	Normalized injection length for different values of α . Solid line indicates the theory. Figure adapted from [13].	16
2.1	Photograph of full experimental apparatus.	18
2.2	Injection platform that slides inside the rotating assembly.	20
2.3	Computer assisted design model of rotating assembly with injection platform inside.	21
2.4	Photograph of the rotating assembly with injection platform inside	21
2.5	Graph over five seconds of the rotation speed of the AC motor that turns the rotating assembly. Green line indicates command velocity, white line indicates actual velocity.	24
2.6	Square wave to represent the injection speed of the rod over time. The period of this example is 4 seconds with an amplitude of 1 centimeter per second. The duty cycle is 50% for this waveform.	30
3.1	a.) Shows a top and side view of the VPS rod in a helical initiation state. b.) Shows a top and side view of the VPS rod in a straight state after being in a helical state	33
3.2	Release time for a rod rotated at different speeds after experiencing helical initiation at $l_h = 79.11 \text{ cm} \pm 5.67 \text{ cm}$. Release time does have a dependence on rotation speed up to $\omega = 35 \text{ RPM}$ for a rod in the static case.	34
3.3	Log-log plot of release time for a rod rotated at different speeds after experiencing helical initiation at $l_h = 79.11 \pm 5.67$ centimeters. The power law fit line follows $t_R = 75.2 * \omega^{-0.895}$. This function yields an R^2 value of 0.97.	35

3.4	Release times measured for various helical initiation lengths. The rotation speed of the assembly was 60 RPM in order to cause the rod to change from a helical to straight state. The linear fit of this plot with 95% confidence is $R_t = (0.059 \pm 0.011)L_H - (2.84 \pm 1.50)$. This function yields an R^2 value of 0.705.	36
3.5	Length of rod injected into the tube before helical initiation (red circle) and lock up length (black circle) as a function of the period for on-off injection. All experiments injected the rod at $v_i = 1 \frac{cm}{sec}$ and rotated the assembly at $\omega = 60$ RPM.	38
3.6	Length of rod injected into the tube before helical initiation (red circle) and lock up (black circle) normalized by the results from the static case as a function of the period for on-off injection. All experiments injected the rod at $v_i = 1 \frac{cm}{sec}$ and rotated the assembly at $\omega = 60$ RPM.	38

Chapter 1

Introduction

1.1 Motivation

The buckling of thin elastic rods while undergoing insertion into a cylindrical constraint arises in many systems, such as vascular catheters [1] and coiled tubing operations in the oilfield [12]. The catheter and coiled tubing are both classified as slender rods because their lengths are much greater than their diameters. The goal of this study is to increase the distance that a rod can be inserted into a cylindrical constraint before “lock-up” occurs. Lock up is defined as the point at which applying a force to inject the rod will no longer move the rod forward through the cylinder. This will be discussed more in depth in §1.2.

Increasing the reach of a rod injected into a cylindrical constraint is important for coil-tubing operations in the oil and gas industry, where a slender steel pipe (approximately 10cm diameter and 10 km length) is inserted into the horizontal section of a wellbore for servicing [15]. In the past ten years, there has been a drastic increase in the number of active rotary drill rigs in North America drilling horizontal wells [6]. The GSF Rig 127 by Transocean drilled the longest horizontal well to date, measuring 11,569 meters in horizontal length [2]. Servicing these long wells requires the slender pipe to have a very long reach. Currently, the rods being inserted into the wellbores can only reach approximately three kilometers out of the eleven kilometers wellbores [16]. Thus, a 370% increase in lock up length can make an important impact on the industry by

allowing for the entire length of the well to be serviced after drilling. Utilizing the entire segment of the horizontal well leads to an increase in efficiency, thus leading to increased profits and energy for society.

1.2 Previous Work

1.2.1 Compression of a Rod inside a Cylinder

Many previous studies have investigated the compression of a fixed length rod inside a cylinder [3, 4, 7]. This relates to the case being studied in this paper because compression of a rod inside a cylinder explores the stresses that are built up when a rod is injected into a cylinder due to the mass of the rod and friction between the rod and cylinder. As the rod is progressively compressed it goes through three configurations: i) straight, ii) sinusoidal buckling, and iii) helical buckling (which with further stress leads to lock up). These three configurations are shown in figure 1.1.

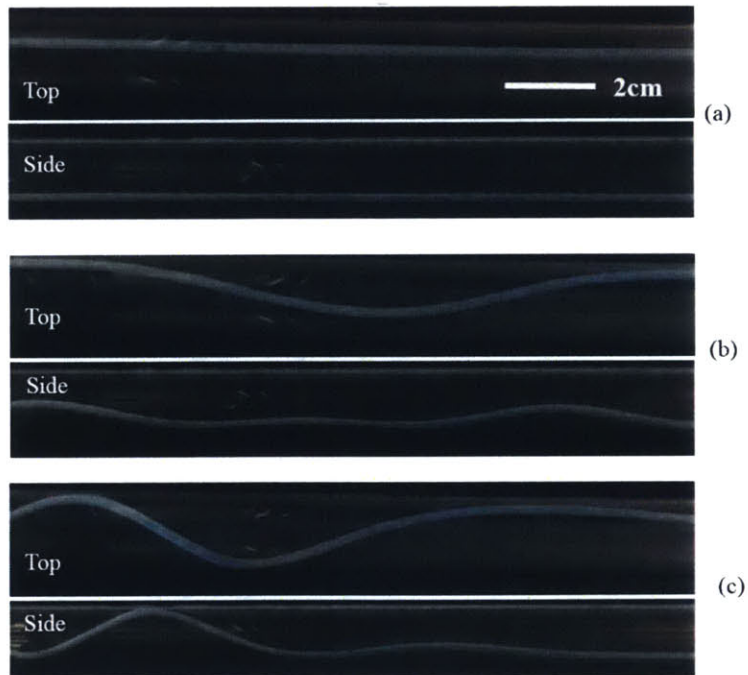


Figure 1.1. a.) Rod in a straight configuration b.) Rod in sinusoidal configuration c.) Rod in helical configuration

The first case to examine is the onset of the sinusoidal state. Paslay and Bogey [14] derived the formula,

$$P_{cr}^s = EI\left(\frac{n\pi}{L}\right)^2 + \frac{w}{\Delta r} \left(\frac{L}{n\pi}\right)^2 \quad (1)$$

where P_{cr}^s is the critical force at which the rod buckles into a sinusoidal state, E is the Young's Modulus of the rod, I is the inertia of the rod, n is the number of half wavelengths of the buckled rod, L is the rod length, w is the buoyant weight of the rod per unit length, and Δr is the radial clearance between the rod and the cylinder. Although a buckled configuration, the sinusoidal shape still allows the rod to continue to inject into the cylinder.

The next case to examine is the helical state. This occurs after the axial load grows sufficiently past P_{cr}^s , which has been derived by Chen, Lin, and Cheatham [4] to result in equation 2.

$$P_{cr}^h = 4EI\left(\frac{m\pi}{L}\right)^2 + \frac{w}{2\Delta r} \left(\frac{L}{m\pi}\right)^2 \quad (2)$$

where P_{cr}^h is the critical force in which the rod buckles into a helical state and m is the number of full pitch lengths of the helical shape.

Different literature suggests various formulas for the critical buckling load [5, 11, 17] that have all been derived with different methods. Equation 2 is explicitly mentioned in this thesis because it is used to derive expressions in future sections. The work above assumes a frictionless interaction between the rod and the cylinder.

1.2.2 Static Injection

While the compression of a rod into a cylindrical constraint gives us a starting place for exploring this topic, the injection of a rod must be explored next since it is a direct scaled down version of

the field case in the oil industry, meaning the configurations are heterogeneous. Injecting the rod into a cylindrical constraint consists of applying an axial force to the rod at the point where it enters the cylinder. The force required to inject the rod increases as the amount of rod inside the cylinder increases. This is due to the increase of mass being pushed forward and the increase in length of rod in contact with the constraint thus resulting in higher frictional forces in the axial direction. As discussed in §1.2.1, the injected rod starts in a straight, unbuckled configuration, buckles into a sinusoidal configuration, followed by a helical configuration, and eventually reaching a critical helical state where the rod locks up and cannot be injected any further. The stresses built up in the rod during lock up can destroy the rod, or specifically coiled the tubing inside the wellbore in the field, thus resulting in critical damage.

An equation to determine the length at which the sinusoidal state occurs, found by McCourt et al. [8], is given by,

$$L = 7.83 \sqrt[3]{\frac{EI}{\mu w}} \quad (3)$$

where μ is the frictional coefficient between the rod and the cylinder. This theory assumes the sinusoidal buckling to be independent of the radial clearance between the rod and the cylinder. This assumption is absent in the analysis in §1.2.1.

McCourt et al. also determined the critical helical buckling length to be

$$L_{inj}^{hel} = \frac{3\sqrt{2}}{\mu} \sqrt{\frac{EI}{w\Delta r}} \quad (4)$$

which shows that the helical buckling length has an inverse dependence on friction. The square root relationship between length and the rod property parameters matches with the analysis done in the previous section.

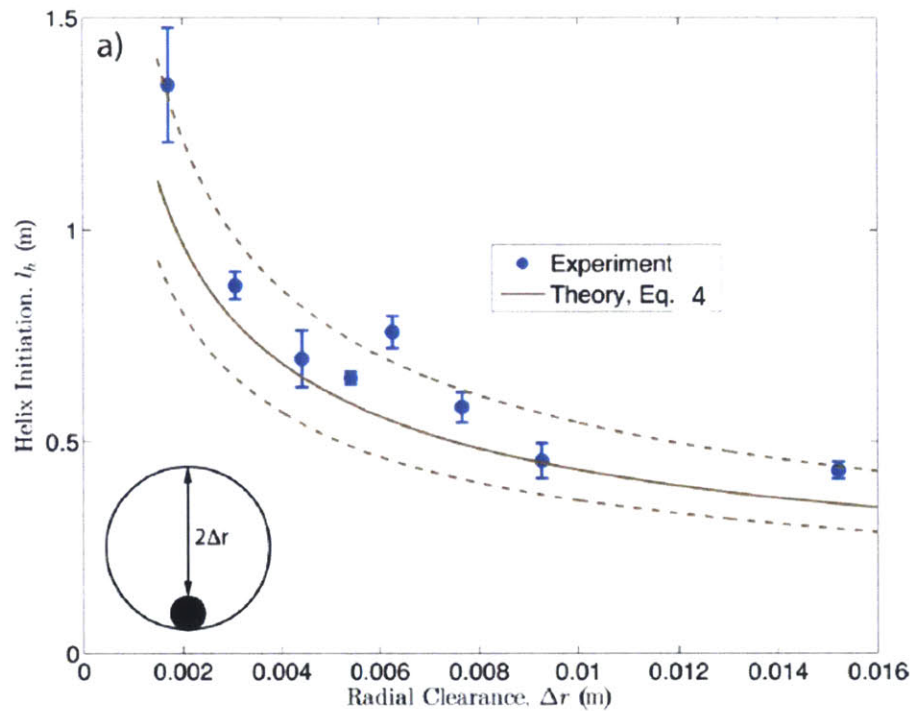


Figure 1.2. Helix initiation length compared to radian clearance. Radian clearance is depicted in the bottom left of plot. Figure adapted from [10].

To further explore this topic, recent experiments have been performed at the EGS Lab at MIT to gather data for comparison with the theories described above. The experiments examined the relationship between the radial clearance of the cylindrical constraint and the measured length at which the rod helically initiated. The equation (Eq. 4) for this theory is shown by the solid line in figure 1.2. The data found in these experiments support the mathematical theory. In future sections we will look at methods to increase the length before lock up in order to maximize reach.

1.3 Rotation Injection Theory

In order to increase reach, energy can be added to the system by continuously rotating the rod relative to the cylinder. This method, developed by Dr. Tianxiang Su (Schlumberger), is accomplished by rotating the injection set up. The rotation propagates throughout the rod, causing the rod to climb up the pipe as shown in figure 1.3. Climbing up the pipe to some angle theta reduces the frictional force since the normal force is no longer in the vertical direction, as shown in equation 5, thus allowing the rod to inject further.

$$F_N = mg \cos(\tan^{-1}(\theta)) \tag{5}$$

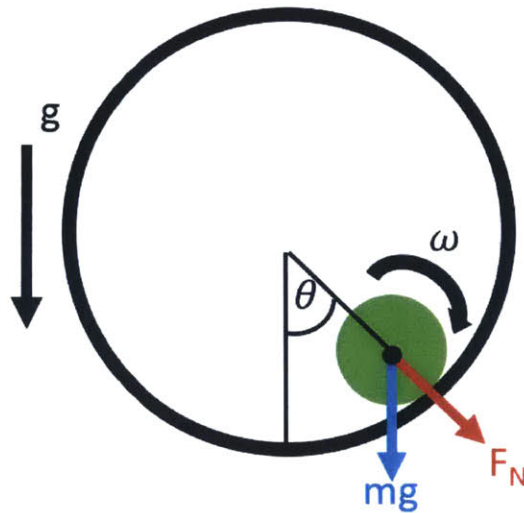


Figure 1.3. Axial view of the rod inside a cylinder. Gravitation force pushes down, but normal force is at an angle relative to the vertical axis.

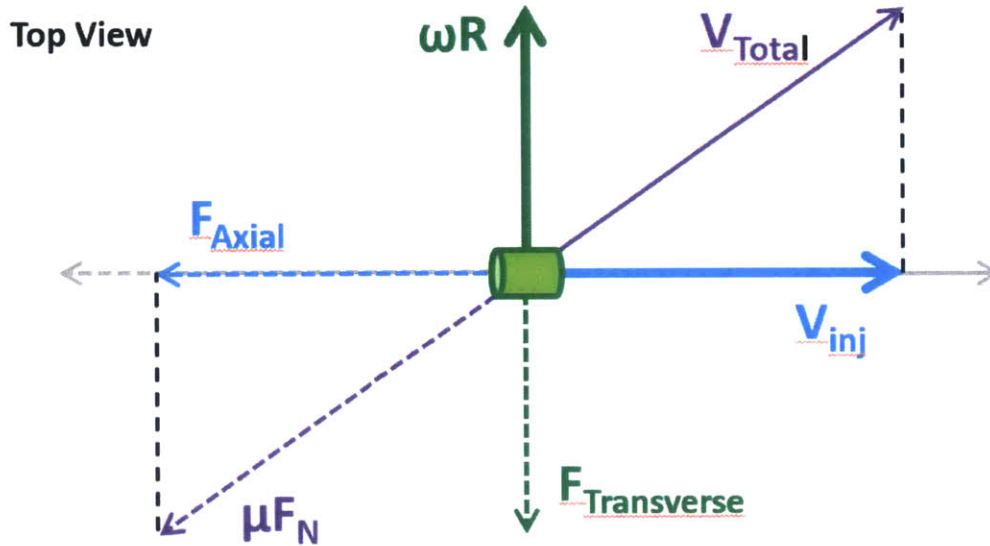


Figure 1.4. Top view of the forces acting upon the rod as it moves through the cylindrical constraint. Figure adapted from [13]

As depicted in figure 1.4, the rotation of the rod adds a velocity component perpendicular to the direction of injection. This results in a velocity vector that does not point axially along the rod, unlike the velocity vector for the rod in the absence of rotation. The friction between the rod and the cylinder remains constant and opposes the perpendicular velocity component. The axial component of the frictional force is responsible for buckling, and this axial component of friction is reduced due to the transverse frictional force causing the frictional force to be at an angle, thus reducing the axial frictional force on the rod.

This reduction in friction due to both the rod climbing the cylinder and the new velocity component helps the rod move further into the pipe before helix initiation occurs. Thus, we expect that faster rotation will lead to longer injection lengths before helix initiation and lock up. The two friction force reductions can be combined with earlier equations to create the following theoretical prediction for the helical buckling length with rotation given by,

$$L_H = \sqrt{1 + (1 + \mu^2)\alpha^2} L_H^0 \quad (6)$$

where,

$$L_H^0 = \frac{3\sqrt{2}}{\mu} \sqrt{\frac{EI}{w\Delta r}} \quad (7)$$

and,

$$\alpha = \frac{\omega r}{v_{inj}} \quad (8)$$

Equation 7 is the length of helical initiation for the static case where the rod is not rotating. The μ in equation 6 is the coefficient of friction in the tangential direction rather than in the axial direction. Additionally, the parameters that affect α in equation 8 are ω (angular rotation speed), r (radius of the rod), and v_{inj} (velocity at which the rod is injected into the cylinder). These formulas will be used in §1.3.1 to compare the experimental results against these theoretical formulas.

1.3.1 Rotation Injection Experiments

The effect of rotation on the injection of a rod into a cylindrical constraint was recently investigated by Connor Mulcahy under the supervision of Professor Reis. Through the use of the set up (see §2.1) that was in part designed and built by the author, an elastic rod was injected into a borosilicate tube while rotation of the rod occurred at the injection site.

Figure 1.5 shows helical buckling length normalized by the static buckling lengths for different values of the dimensionless parameter α , which is defined in equation 8. The static buckling length is defined as the length at which buckling occurs for a rod that undergoes no rotation and constant injection speed. The data in figure 1.5 shows that with a high value of α , the length to helix initiation can be increased by up 500% (at $\alpha = 6$).

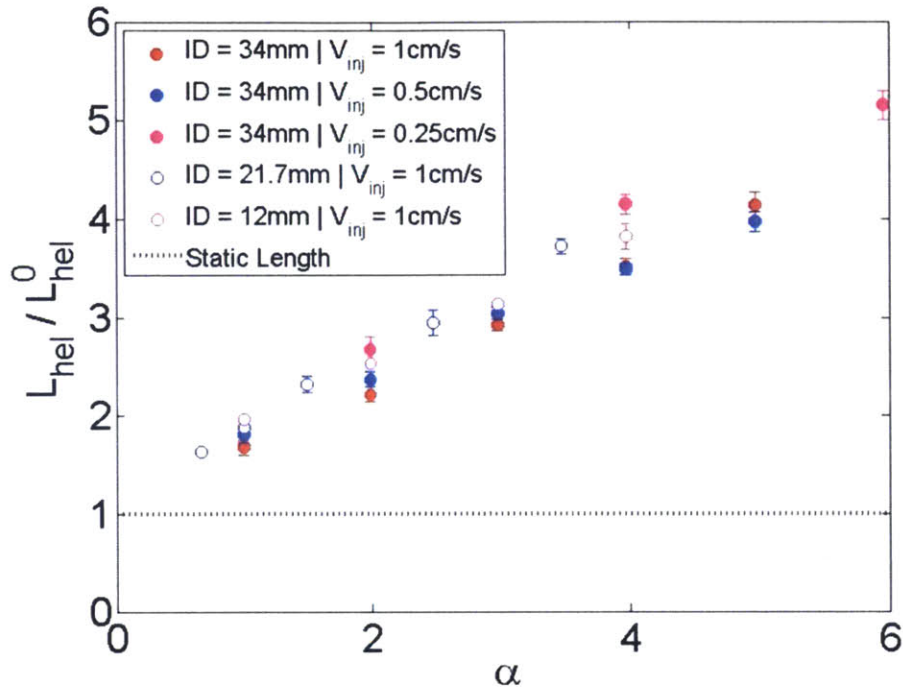


Figure 1.5. Normalized injection length for parameter α . Data collected for different radial clearances. Figure adapted from [13].

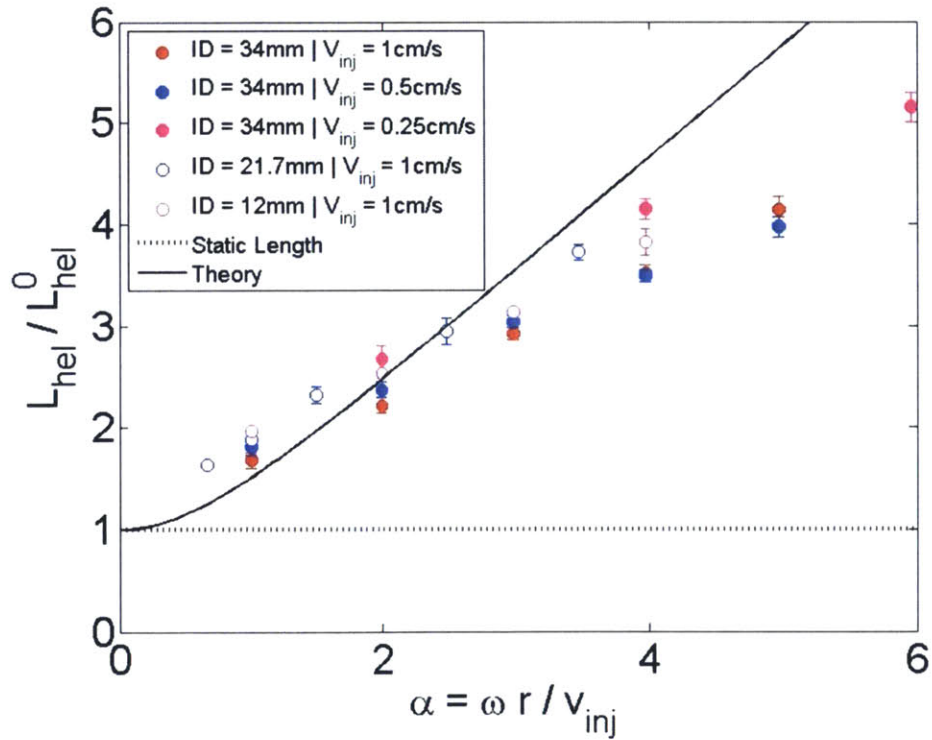


Figure 1.6. Normalized injection length for different values of α . Solid line indicates the theory. Figure adapted from [13].

The data in figure 1.6 appears to undershoot the theory. This may be due to the torsion created in the rod which decreases the amount of force required to enter a helical state. Despite the slight difference, the theory validates the physical experiment. This gives us confidence moving forward to collect and analyze data with other rotation-related experiments, such as rotating with on-off injection.

1.4 Rotation with On-Off Injection

During previous experimentation it was observed that once the rod has entered the sinusoidal configuration without rotation, it could be reverted back to the original straight configuration by rotating the rod at the injection site. By rotating the rod at the injection site, a torque is applied throughout the rod, thus causing the entire length of the rod to rotate. Once the rod has returned to a straight configuration, it can be continued to be injected to a point that reaches further than the lock up length as compared to the condition without rotation.

This thesis aims to further explore the on-off injection by first measuring how long it takes for different rotation speeds to restore the rod to a straight state after helically initiating. This data will then be used to determine the required amount of “off” time to optimize injection and increase the length of injection before lock up. The goal is to increase reach by at least 450% since this is the amount of increase required to service the entire wellbore in the field case.

Chapter 2

Experiment

2.1 Experiment Apparatus Design

In this experiment, a 3.65 meter long borosilicate pipe and a rotating injection assembly were constructed, as shown in figure 2.1. An elastic rod was injected into the borosilicate pipe to simulate a metal rod inserted into a horizontal wellbore. The primary parameters that were changed were rotation speed, helix initiation length, and period of injection duty cycle. Each trial consisted of injecting a rod and rotating the assembly. The tube was required to be cleaned and the rod had to be treated with chalk after every five trials in order to maintain a consistent friction coefficient between the rod and the constraint. Injection speed was set at one centimeter per second for all trials. A camera was mounted above the injection site to record videos of all experiments. These videos were analyzed to measure the length of rod injected into the tube and the time required for the rod to enter different states. The components that make up this experiment apparatus are described below.

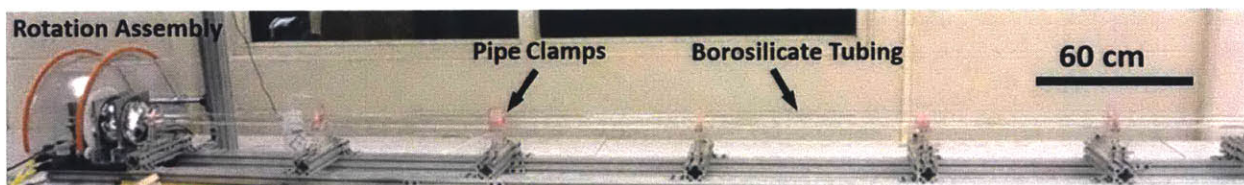


Figure 2.1. Photograph of full experimental apparatus.

2.1.1 Injection Platform

The injection mechanism for the rod is composed of a stepper motor¹ with a drive wheel on the shaft and a free rotating wheel. Six quarter-inch acrylic layers create the support for the motor and rotating wheel as well as a gap for the elastic rod to fit through. Each of these acrylic layers were laser cut to ensure precision. The drive wheel and free rotating wheel grip the elastic rod and then insert it by controlled rotation of the drive wheel. The stepper motor rotates using Labview software with closed loop feedback. Before any experiments were performed, the motor controller was calibrated for the user to easily input and change injection speed values with units of centimeters per second. The Labview program has also been programmed to allow the stepper motor to turn on and off at different duty cycles and frequencies.

The injection platform sits inside the rotating assembly, with the axis of rotation being about the gap for elastic rod injection. Counterweights were added to the opposite side of the rod spool to bring the center of mass closer to the axis of rotation. This is to minimize the variation in the torque required to continuously rotate the assembly at a constant rotational velocity. The counter weights are composed of eight four-millimeter screws with three ten millimeter nuts on each screw. According to computer assisted design software, the center of the mass in this set up is roughly two centimeters away from the center of rotation. Given that the diameter of the rotating assembly is approximately fourteen centimeters, the distance between the center of mass and center of rotation does not cause significant variation in torque.

¹ Intelligent Motor Systems MDrive 14 Plus Motion Control, with 51200 steps per revolution and 2048 edges per revolution resolution (internal encoder).

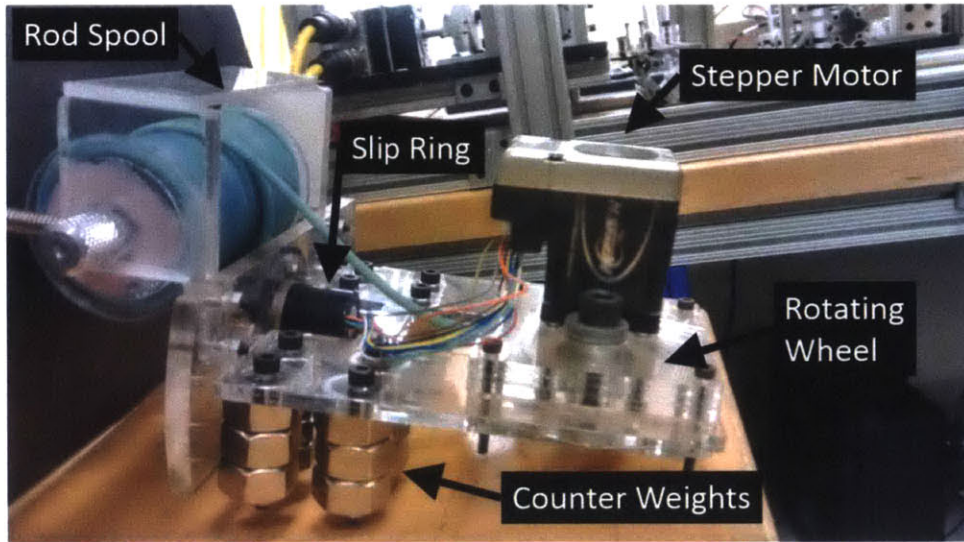


Figure 2.2. Injection platform that slides inside the rotating assembly.

The rod spool sits on the end of the injection platform. The design and purpose of the rod spool will be discussed more in §2.1.3. An eight wire slip ring² allows power and electronic signals to be carried from the computer and electrical outlet to the stepper motor. The wires are longer than the distance from the slip ring to the stepper motor input, thus they naturally buckle and do not collide with the elastic rod.

2.1.2 Rotating Assembly

The injection platform described in §2.1.1 can slide into a 5.5 in inner diameter acrylic tube. A removable plate on the back of the acrylic tube prevents the shelf from sliding out axially during rotation. As shown in figure 2.4, there are two rotary ball bearings³ press fit around the acrylic tube that are constrained by two aluminum bearing mounts. Each motor mount has two quarter inch set screws to constrain the ball bearings axially.

² Adafruit Slip Ring with Flange, 8 wires, max 240V at 2 amps per wire. Can spin up to 300RPM.

³ Ultra-Thin Multi-Load Stell Ball Bearings, rotate up to 333RPM and has a dynamic torque capacity of 2,240 inch pounds.

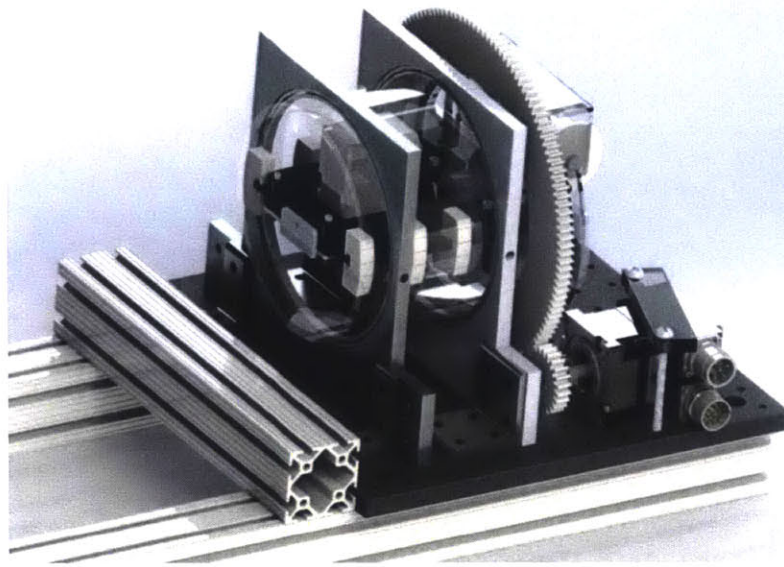


Figure 2.3. Computer assisted design model of rotating assembly with injection platform inside.

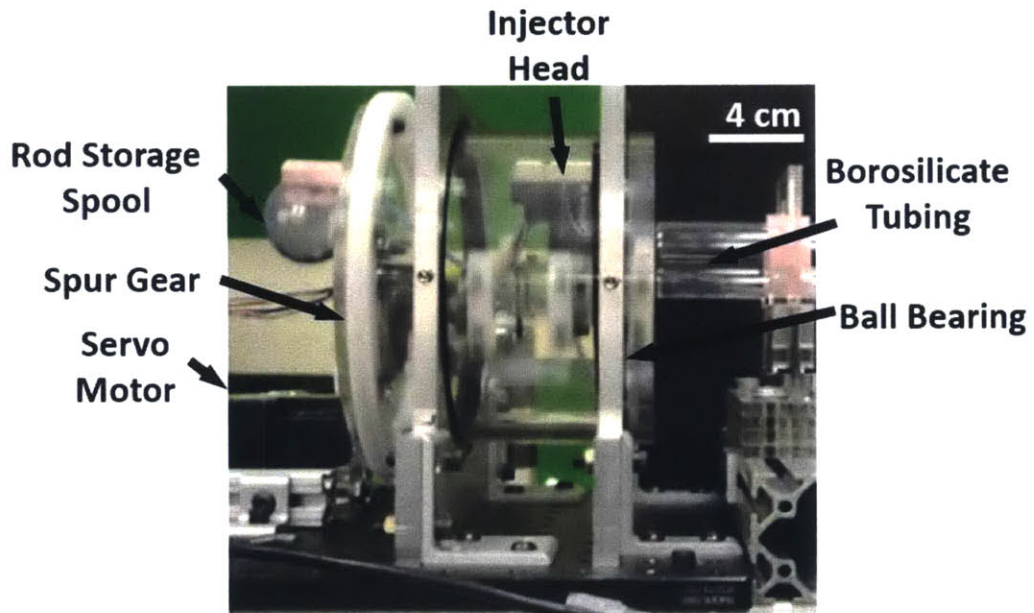


Figure 2.4. Photograph of the rotating assembly with injection platform inside.

The set screws cannot be turned too tightly because this deforms the circular shape of the tube and bearings into an ellipse, thus increasing friction in the ball bearings and decreasing consistent rotation. The bearings allow for a maximum rotation speed of 300 RPM, which sets the limit on rotation speed of the assembly.

Around the back of the acrylic tube is a 132 tooth, 20 degree pitch spur gear composed of acetal resin. Acetal resin was selected because it is both light and durable. The spur gear was fabricated in three separate parts on a computer numeric controlled micro-milling machine. The large spur gear is driven by a 24 tooth acetal resin gear mounted onto an AC servo motor, thus the gear ratio between these two gears is eleven to two. The AC servo motor will be described in more detail in §2.1.5.

2.1.3 Rod Storage

In order for the rod to not become twisted before entering the tube, it must rotate with the injection site. This requires a significant length (4 m) of elastic rod to both rotate with the acrylic cylinder and continuously inject with minimum resistance on the stepper motor. A spool mounted on the back of the acrylic cylinder design was chosen to accomplish this goal. The diameter and length of the spool were chosen in order to minimize the size required for the spool and rod. This was calculated with simple geometry and the requirement that the elastic rod must be 425 cm long and have a diameter of 0.5 cm.

$$SA_{required} = 425 * 0.5 = 212.5 \text{ cm}^2 \quad (9)$$

$$SA_{spool} = 2\pi d \quad (10)$$

In the two equations above, SA is defined as surface area. The equation is multiplied by two to show that the rod can wrap around the spool twice before it is considered too thick. The spool can be a maximum of nine centimeters long given the size of the acrylic tube, thus the spool will be nine centimeters long in order to minimize the required diameter.

$$212.5 \text{ cm}^2 = 2(9)\pi d \rightarrow d = 3.75 \text{ cm} \quad (11)$$

This diameter in equation 11 is roughly 1.5 in, thus a 1.5 in piece of acrylic tube was used for the rod storage spool. A quarter inch hole was drilled through the center to allow for an aluminum pin to slide through the center of the spool and hold it in place. This pin is held in place with a set screw. The spool required guards on each side to ensure the elastic rod did not slip between the spool and the mount holding the spool in place. These guards were adhered onto the spool with acrylic solvent, a special adhesive that breaks down the acrylic to fuse it back together as the liquid evaporates.

2.1.4 Borosilicate Tubing

A borosilicate pipe was used to create the cylindrical constraint. This material was chosen because it is easy to clean, smooth, and transparent. Each length of borosilicate pipe is approximately 120 cm long. The set up requires three pipes of equal diameter set in a line to build a cylindrical constraint long enough to run experiments.

Each section of pipe is supported by three laser-cut acrylic stands to ensure that each pipe is of equal height and level with respect to one another. At the clamping point of the stands, a thin rubber ring wrapped around the pipe is used to dampen any potential vibrations. A 300 g weight is placed on top of each clamp when fastening to create the same amount of pressure at each clamping point. All experiments discussed in §3.1 use pipes with an inner diameter of 21.7 mm. As shown in the introduction, the pipe diameter was changed in order to show the relationship between injection length to lock-up and radial clearance between the rod and cylindrical constraint. This is important to review to confirm that the data matches the theory and to understand the relationship between injection length and clearance for the field case.

2.1.5 AC Motor and Electronics

An AC servo motor⁴ was used to drive the rotating assembly. As stated in §2.1.2, the AC motor shaft was connected to a 24 tooth acetal resin gear. The motor is constrained by an acrylic bar being pressured down to the top of the motor. This design allows for the motor to be easily moved for improving gear meshing. To drive the motor, a Xenus amplifier with a controller network area (CAN) bus was used. This amplifier works with the control software, CME 2 from Copley Controls. The controller allows angular velocity and current to have position and integral control used on them and angle to have position and derivative control used. Values for each of these control parameters were found by starting with the recommended values and then slowly adjusting them as needed by monitoring the output on an oscilloscope to tune the controller. An example of the input control (green line) and the output angular velocity (white line) is shown in figure 2.5.

Since the stepper motor is positioned inside the rotating assembly, a slip ring was used to transmit power and signals from the rotating assembly to the computer. Both motors were controlled from the same computer during experiments.

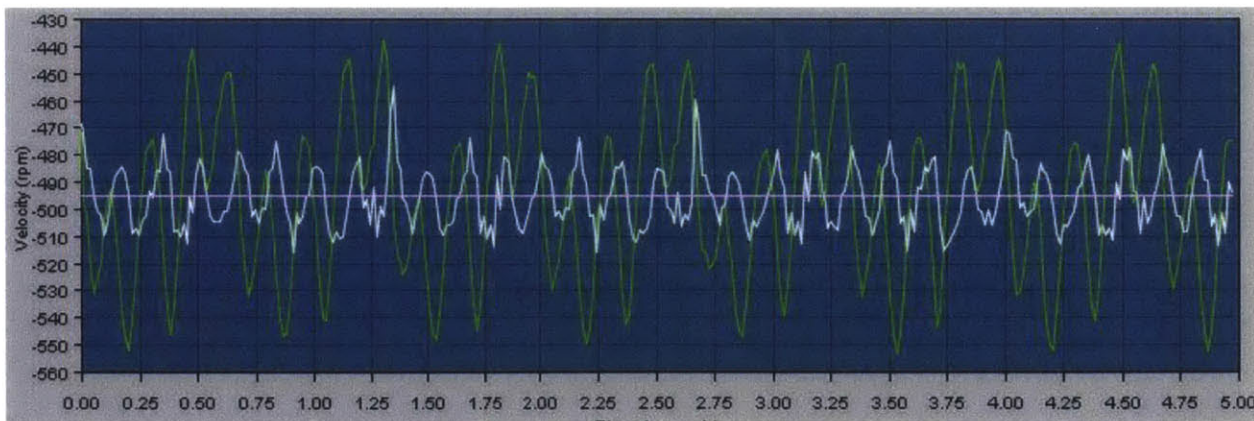


Figure 2.5. Graph over five seconds of the rotation speed of the AC motor that turns the rotating assembly. Green line indicates command velocity, white line indicates actual velocity.

⁴ Parker Motion BE230F DC Motor, Stall torque of 0.37 Nm, Rated speed of 5000 RPM.

2.2 Experiment Preparation

The elastic rods used for this experiment were custom fabricated. Since the curvature of the rod needs to be a controlled parameter in the samples, a method for rod fabrication had previously been developed [9]. The rods are fabricated within the lab rather than purchased because commercial rubber rods are typically extruded and then wrapped around a spool for transport and storage, giving the rubber rod a natural curvature. For this experiment, the rubber rods consistently need to have no natural curvature.

An injection molding process was used to fabricate the rod. The mold for this rod was a 4.25 m 3.16 mm ID PVC tube held straight by being fixed to a long aluminum extrusion. The material for the rod is a vinylpolysiloxane (VPS) polymer⁵. To make this polymer, a liquid base and liquid catalyst are mixed together. The polymerized liquid then has a working time of 10 minutes and a setting time of 30 minutes at room temperature. Within this 10 minute working time window, the polymerized liquid is injected into the PVC tubing with a syringe. After allowing the polymer to set inside the tube for at least an hour, the PVC tubing is carefully cut away to release the VPS elastic rod. The rod is then left to set for a week before use in experiments to allow the mechanical properties to stabilize. After this period, the rod has a Young's modulus of 1290 ± 12 kPa, a density of $1200 \frac{kg}{m^3}$, and a radius of 1.57 mm.

To maintain consistent frictional conditions throughout the experiment, the rod and tube were cleaned after every five trials. The cleaning process for both of these objects are described below in §2.2.1 and §2.2.2.

⁵ Elite Double 32, a Vinylpolysiloxane material manufacture by Zhermach is the rod material.

2.2.1 Rod Cleaning Process

Since friction is an important factor in determining rod buckling lengths in this experiment, the surface properties of both the rod and tube need to be consistent between all experiments. The cleaning process for the rod and tube involved treating the surfaces of these two objects.

To create consistent frictional coating, the rod was first coated in Irwin Strait Line Marking Chalk by placing the rod in a small container full of the chalk and shaking this container for one minute. The rod was then sent through a small tube with fast moving air inside in order to blow loose chalk off of the rod. Last, the rod is placed between chalk board erasers and pulled out to create an even coating of chalk. The rod is carefully placed on clean surfaces throughout the process in order to keep particles from sticking to the rod and affecting the chalk coating. Once the rod was cleaned, it was wound around the spool that attached to the back of the rotating set-up. When not in use, the rod was taken off the spool and laid out flat on a table to prevent a natural curvature to be applied to the rod.

2.2.2 Tube Cleaning Process

The interior of the tube becomes dirty from the rod surface leaving chalk residue behind as well as dust particles floating into the tube. In order to remove this residue and dust, a thick flexible plastic rod was threaded from the start to the end of the tube first. An ethanol soaked paper towel was then attached to a hook on the plastic rod located near the injection site. This towel was slightly larger than the diameter of the borosilicate tube, thus the ethanol wipes the entire surface inside the tube. Next, the plastic rod was pulled from the exit site so that the ethanol towel started at the injection site and passed through the entire tube. Once the ethanol towel exited the tube, the same

process was repeated but with a cloth attached to the plastic rods hook instead of the ethanol towel. This wiped much of the ethanol, dust, and chalk up off of the interior tube surface. Finally, air flow was sent from the injection site to the end of the tube. The air flow was left for three minutes to ensure the interior of the tube is dry and all ethanol has evaporated. The cloth was used for multiple cleaning processes, but the ethanol towel was switched for every cleaning process.

2.3 Data Acquisition

As stated earlier, data for this experiment relates to a rod being injected into a cylindrical constraint while the rod undergoes rotation. Different aspects of rotation and injection were explored through experimentation in order to quantify methods for increasing the lock-up length. The procedures followed for experimentation are describe in §2.3.1 and §2.3.2. All of these procedures follow the design preparation, rod manufacturing, and cleaning processes. The experiments also maintained a constant radial clearance between the rod and cylindrical constraint.

2.3.1 Release Time Experimentation

As discussed in §1.4, a rod in a cylindrical constraint that reaches a sinusoidal or helical bucking state can be reverted back to a straight state by rotating the rod at the injection site. The release time is defined as the amount of time required for the rod inside the cylinder to change from a helical state to a straight state. The aim of release time experimentation was to determine the amount of time required for the rod to transition from the helical bucking state to the straight state at different rotation speeds and different helical bucking lengths.

To determine if the release time is dependent on rotation speed, the VPS rod was first injected into the borosilicate tube with no rotation at the injection site, also known as static case injection. The injection speed was one centimeter per second, although previous work from §1.2.2 shows that the helical initiation length for the static case does not have any injection speed dependence. The rod injection would be stopped by the experiment operator once helical initiation occurred. The experiment operator then turned on the DC motor with a set rotation speed, thus rotating the rod inside the tube and causing it to exit the helical state and enter the straight state. The experiment was complete once the rod rested approximately straight at the base of the tube. This procedure was repeated for multiple rotation speeds.

To determine if the release time is dependent on length of rod injected before helical initiation, the VPS rod was first injected to helically buckle at different lengths. To reach the desired helical buckling length, the rod was first injected at one centimeter per second with a continuous injection site rotation speed of 120 rotations per minute (RPM). Since these parameters corresponds to a large α value, the rod would not helically buckle until the rotation was stopped. Once rotation ends past the helical initiation length for the static case, stresses in the rod quickly build up and cause the rod to helically buckle. After a set amount of time, rotation would then be turned off to force helical buckling to occur. The measurement of these different helical initiation points are described in §2.3.3. Once the rod formed a helix, the experiment operator would turn off the injection. The experiment operator then turned on the DC motor causing the injection site to rotate at 60 RPM. This procedure was repeated for multiple helical initiation lengths.

2.3.2 On-Off Injection Experimentation

Once the data were collected to measure release time, experiments were performed to determine the effect of changing the period of on-off injection while maintaining continuous rotation. On-off injection is defined as continuously alternating between starting and stopping the injection of the rod into the cylindrical constraint. On-off injection for these experiments maintained a duty cycle of 50% and an amplitude of 1 centimeter per second. Duty cycle is defined as the amount of time a signal is in an “on” state divided by the period of the signal. By changing the period of the on-off injection, both the on time and off time vary since the duty cycle remained constant. These parameters are shown graphically in figure 2.6.

These experiments were run until lock-up occurred. As discussed in the introduction, lock-up is an irreversible state that rotation cannot change and has the possibility of destroying the rod in real life situations. The on-off injection allows for a rod to enter and exit helical initiation multiple times, thus the lengths recorded were the length at which the first helical initiation occurred and the length at which lock-up occurred.

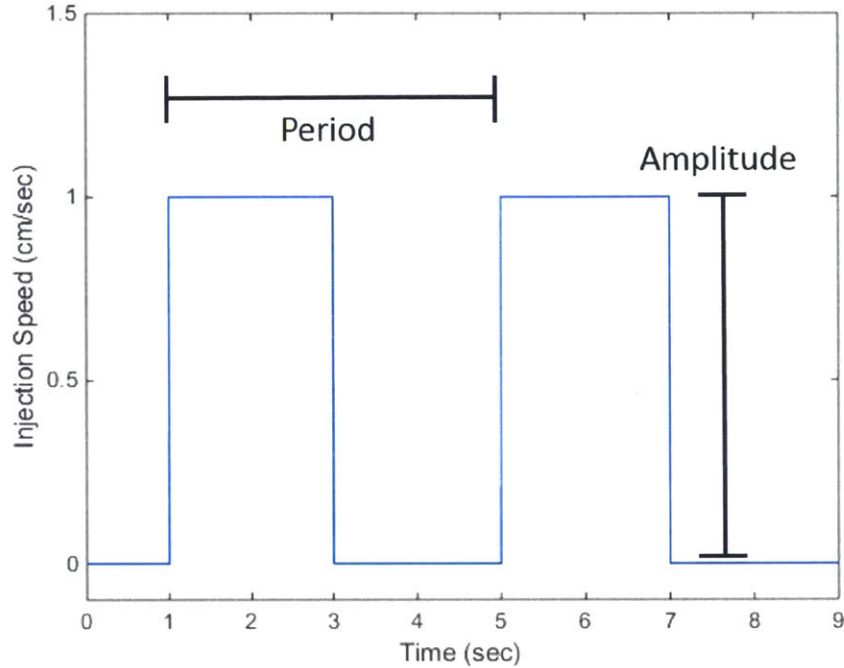


Figure 2.6. Square wave to represent the injection speed of the rod over time. The period of this example is 4 seconds with an amplitude of 1 centimeter per second. The duty cycle is 50% for this waveform.

2.3.3 Video Recording and Analysis

A Logitech webcam was used record the experiments. The webcam was set up 35 cm above the point at which the rod enters the tube. This camera placement was chosen because buckling occurs near this area of the rod. A mirror was placed below the webcam at a 45 degree angle relative to ground in order to allow the webcam to record a top view and a side view of the rod inside the transparent borosilicate tube. Black paper and cardboard surrounded the tube to add contrast between the green rod and background in order to make video analysis easier.

The webcam records at 30 frames per second (FpS). Since the injection speed (v_{inj}) of the rod and frame rate of the camera are known, the length of rod injected into the tube can be calculated by,

$$(f_{end} - f_{start}) * FpS * v_{inj} = L \quad (12)$$

The starting frame (f_{start}) is the frame at which the rod enters the tube and the end frame (f_{end}) is the frame at which the rod reaches the state that length was being measured to. The variable L is the length of rod that has been injected at this point. QuickTime media player software was used to find the frame number for these two points.

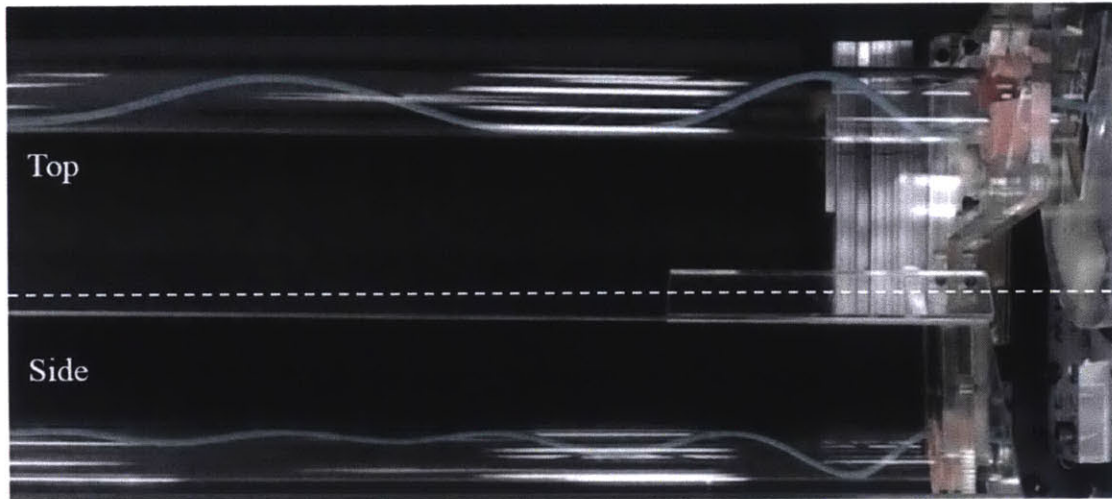
Chapter 3

Analysis and Results

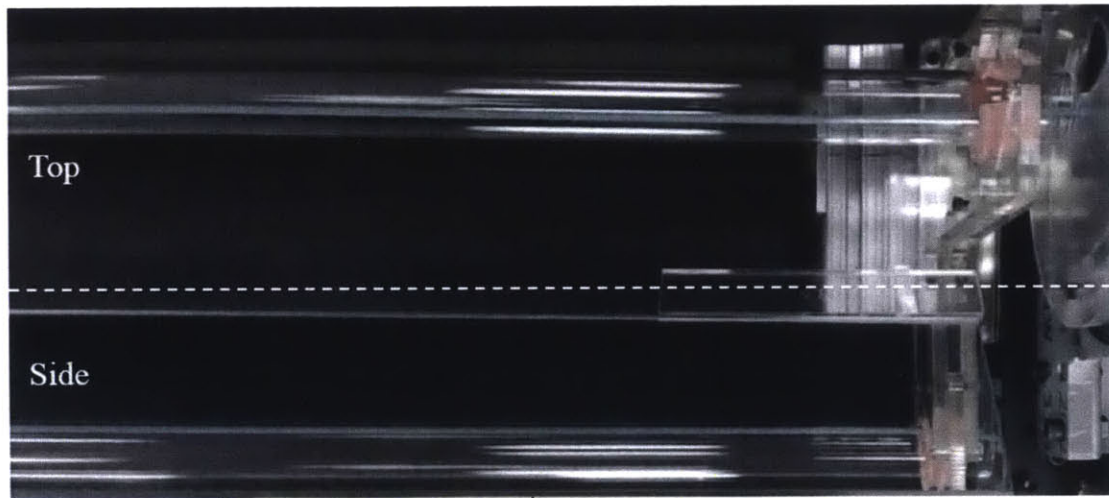
3.1 Release Time

As previously mentioned in §2.3.1, we refer to release time as the time required for the rod to change from a helical state to a straight state. From initial observations, the release time appeared to be dependent on rotation speed and the length of rod injected prior to helical initiation, both of which are address in more detail below.

The release time was measured using video analysis for all trials that explored dependence on both rotation speed and length of rod injected. Figure 3.1 shows a representative example of the first and last frames used to measure the release time. The configuration of the helically initiated rod in the first frame may vary from experiment to experiment because the operator stops the injection manually when helical initiation is seen, which is when the rod touches the top of the tube. Error in the operator could lead to the variance in the data collected for both experiment in §3.1.1 and §3.1.2.



a.



b.

Figure 3.1. a) Shows a top and side view of the VPS rod in a helical initiation state. b) Shows a top and side view of the VPS rod in a straight state after being in a helical state

3.1.1 Dependence of the Release Time on the Rotation Speed

The dependence of the rotation speed on release time was examined for the static case. The total length of rod injected into the tube was measured for each trial. This was done with the method described in §2.3.1. The average length of injection to helical initiation was $l_h = 79.11 \text{ cm} \pm 5.67 \text{ cm}$. The data was collected with rotation speeds varying from 5 RPM to 90 RPM. As mentioned in §2.1.2, the fastest the setup can be made to rotate is 300 RPM, thus the data in figure

3.2 do not quite cover the full range of rotation speeds, but do show a trend for the rotation speeds used. Each data point is the average of five trials.

Figure 3.2 shows that the data asymptotes at approximately two seconds required for the rod to change from a helical configuration to a straight configuration for high rotation speeds and increases significantly at low rotation speeds. This asymptote occurs around $\omega = 35$ RPM. This suggests that there is a limit to the release time due to the physical properties of the system. Video observation showed that the rod stores twist from rotation for a short period of time before the twist translates throughout the entire rod. The time required for the twist to propagate through the entire rod may set a limit on the release time.

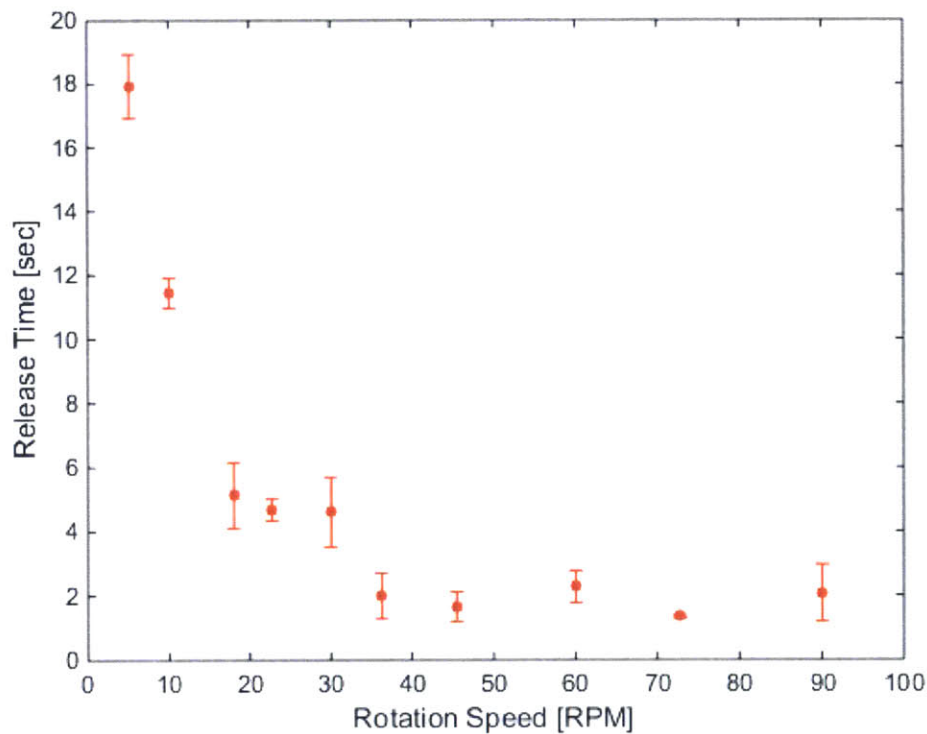


Figure 3.2. Release time for a rod rotated at different speeds after experiencing helical initiation at $l_h = 79.11 \text{ cm} \pm 5.67 \text{ cm}$. Release time does have a dependence on rotation speed up to $\omega = 35$ RPM for a rod in the static case.

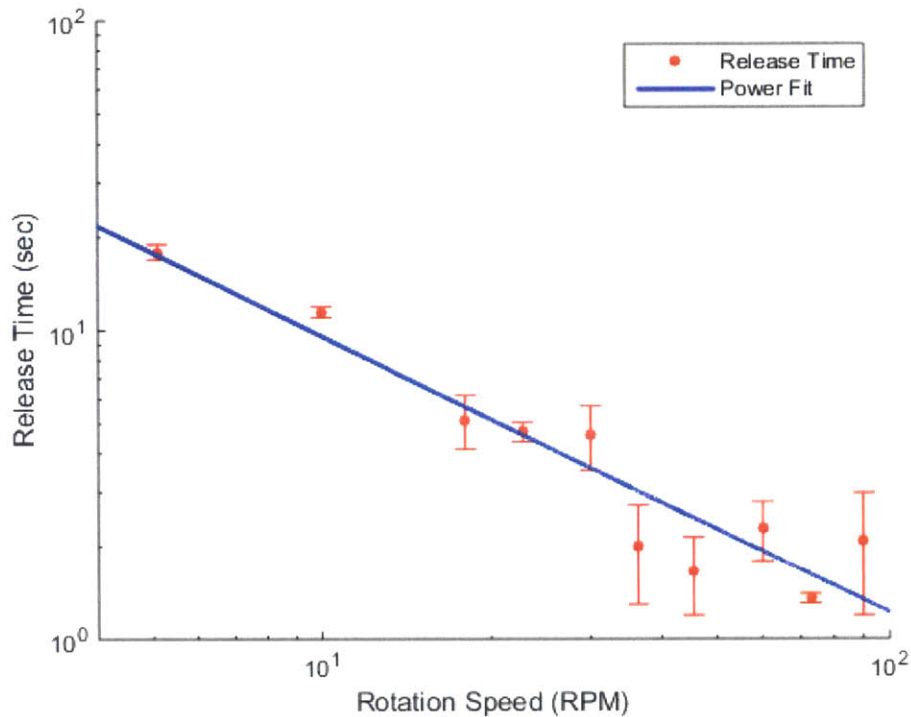


Figure 3.3. Log-log plot of release time for a rod rotated at different speeds after experiencing helical initiation at $l_h = 79.11 \pm 5.67$ centimeters. The power law fit line follows $t_R = 75.2 * \omega^{-0.895}$. This function yields an R^2 value of 0.97.

Since the trend in figure 3.2 appears to be consistent with a power-law, the same data points have been used to plot the data on a log-log graph, as shown in figure 3.3. A power law fit was computed for this data and is plotted above in figure 3.3 as the solid line. The linear fit line is $t_R = (75.2 \pm 0.9) * \omega^{-0.895 \pm 0.249}$, where t_R is the release time and ω is the rotations per minute. This fit has a R^2 value of 0.97, suggesting that the line accurately represents the relationship between rotation speed and release time for a rod that has helically initiated at 75.2 cm.

An important component of the graph is the upper bound on the error bars. The upper bound indicates an estimate of the maximum time required for the rods to change from a helical configuration to a straight configuration at different rotation speeds (assuming a normal distribution). This information can help us set our period for on-off injection by using release time as the time required for the off-time component.

3.1.2 Dependence of the Release Time on Helical Buckling Length

The release times of the rod for at different helical initiation lengths are shown in figure 3.4. To reach these helical initiation lengths, the rod was first injected under a large value of α . Rotation of the assembly was then stopped in order to cause helical initiation. The lengths investigated range from 62 cm to 190 cm. Helical buckling does not occur naturally for lengths shorter than 62 cm for this experimental set up because there is not enough friction to initiate buckling, thus data points could not be collected for any injection length less than this value. All release times were measured with a rotation speed of $\omega = 60$ RPM. Each data point in this plot is an individual trial.

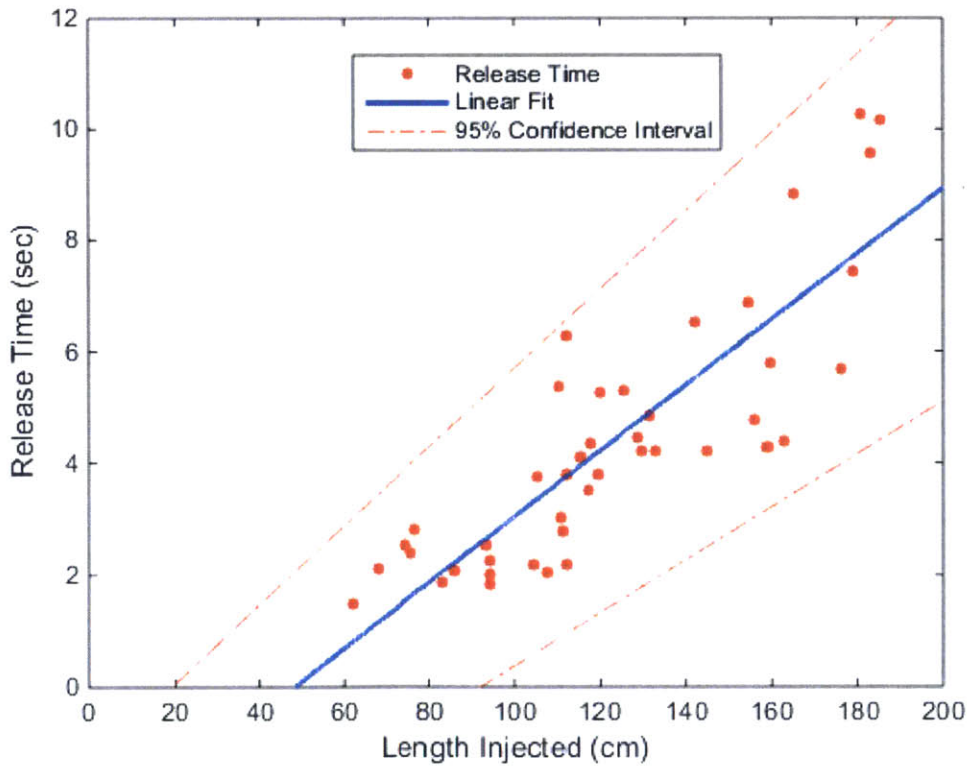


Figure 3.4. Release times measured for various helical initiation lengths. The rotation speed of the assembly was 60 RPM in order to cause the rod to change from a helical to straight state. The linear fit of this plot with 95% confidence is $R_t = (0.059 \pm 0.011)L_H - (2.84 \pm 1.50)$. This function yields an R^2 value of 0.705.

The release times as a function of the injected length plotted in figure 3.4 shows a linear trend with above the threshold value of $l = 47\text{cm} \pm 30\text{cm}$. Since the trend appears linear, a linear fit was applied to this data. The fit has a R^2 value of 0.705 which implies that there is a relationship between release time and length injected, but this relationship is not very strong. The data creates a cone shape, with the point of the cone being near the lower helical initiation lengths. This shape indicates that larger helical initiation lengths will have a more variable release time than lower lengths. Similarly to the data plotted in figure 3.3, the important component of the graph is the maximum release time required for different helical initiation lengths. For example, at 160 cm one would need to stop injection for at least eight seconds to ensure helical buckling would not occur.

3.2 On-Off Injection

The results from the two experiments with on-off injection are shown in figure 3.5. As defined in §2.3.2, on-off injection consists of rotating the injection assembly while the injection speed changes from a positive value to zero at a set frequency and 50% duty cycle. The period of on-off injection acted as the independent variable while both the helical initiation length and lock up lengths were recorded. All experiments were run with an amplitude of $A = 1 \frac{\text{cm}}{\text{sec}}$ and a rotation speed of $\omega = 60$ RPM. Figure 3.5 shows the helical initiation and lock up lengths for the experimental apparatus while figure 3.6 shows the normalized helical initiation and lock up lengths. The data was normalized by dividing the injected lengths by the helical initiation length and lock up length for the static case, which was $l_h = 79.11 \text{ cm} \pm 5.76 \text{ cm}$ and $l_l = 90.20 \text{ cm} \pm 6.21 \text{ cm}$. Each data point and error bar is composed of five trials.

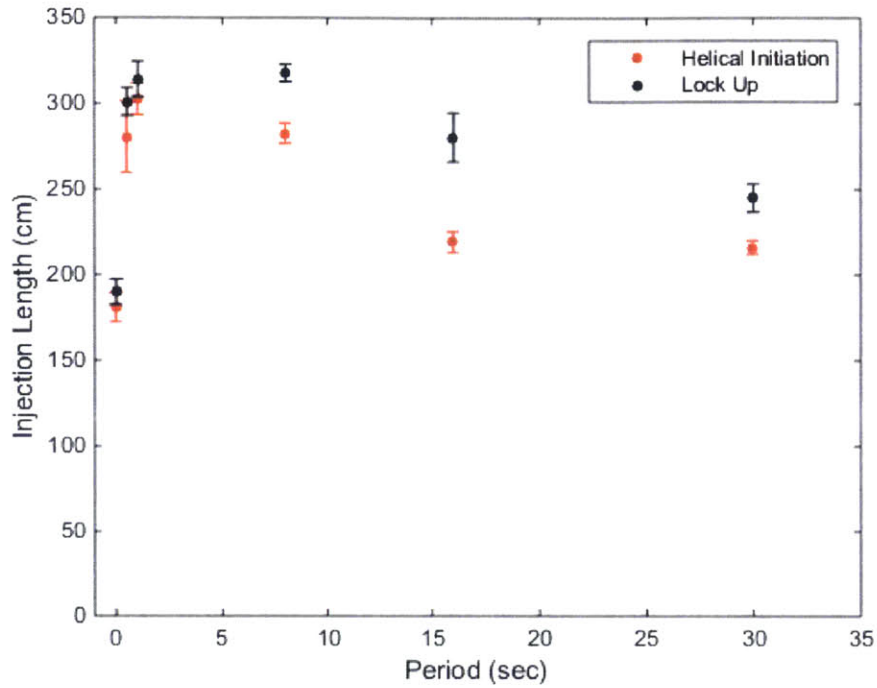


Figure 3.5. Length of rod injected into the tube before helical initiation (red circle) and lock up length (black circle) as a function of the period for on-off injection. All experiments injected the rod at $v_i = 1 \frac{cm}{sec}$ and rotated the assembly at $\omega = 60$ RPM.

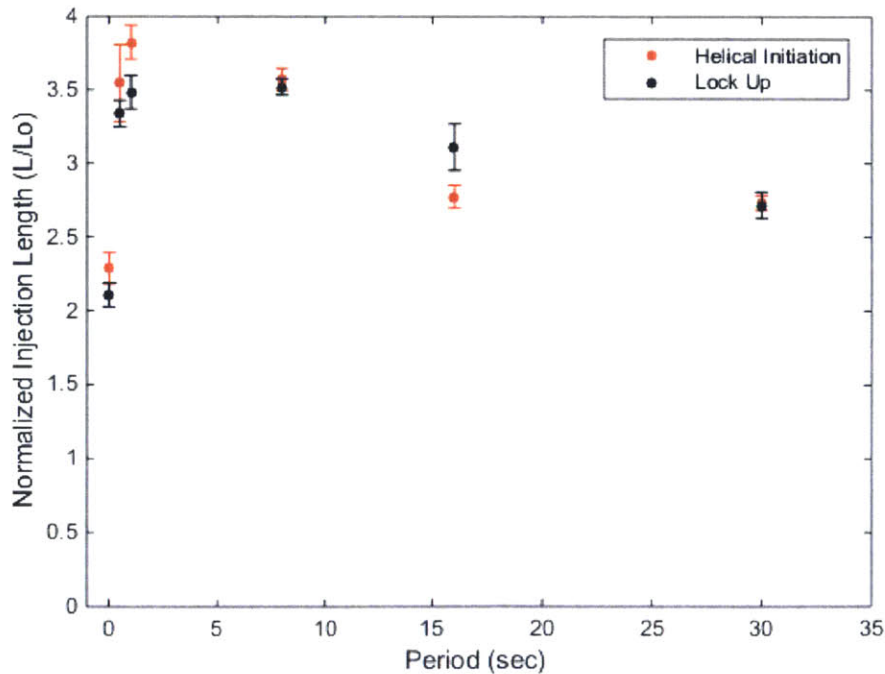


Figure 3.6. Length of rod injected into the tube before helical initiation (red circle) and lock up (black circle) normalized by the results from the static case as a function of the period for on-off injection. All experiments injected the rod at $v_i = 1 \frac{cm}{sec}$ and rotated the assembly at $\omega = 60$ RPM.

Normalizing the data shows that rotating the injection site and using a short period on-off injection signal can increase the helical initiation length by approximately 175% as compared to rotating without using on-off injection. The general trend of both figures 3.5 and 3.6 is that there exists a peak efficiency period for rotation and injection speed (defined as the α parameter discussed in §1.3), the injection length before buckling drastically decreases as the period decreases from this optimal period, and the injection length before buckling gradually decreases as the period increases from this optimal period.

In figure 3.6, the normalized lock up length is sometimes found to be lower than the normalized helical initiation length. This is a result of the difference between the helical initiation length and the lock up length for different conditions. If this difference is small, normalizing these lengths by the static case lengths for helical initiation and lock up causes the normalized lock up length to be lower than the normalized helical initiation length. From figure 3.5, we see that the 16 second period created the greatest distance between helical initiation and lock up. More data collection between the 1 second and 8 second period could provide more information on the injection length peak that appears to be forming. Despite the need to explore more experimentally, the results from these plots show that there is an advantage to using on-off injection.

Chapter 4

Conclusion

For this thesis, we began by designing and constructing a new experimental apparatus comprising a rotational assembly to explore the injection of a rod in a cylindrical constraint. Once this experimental apparatus was constructed, initial experiments were run to observe the effect of rotating the rod on injection length before lock up. This proved to increase the length of rod that could be injected before buckling by at most 500%. Further exploration of the apparatus revealed that switching the injection speed on and off could further increase the reach of the rod. It was found that there exists an optimal period to extend reach for every set of parameters. Periods larger than the optimal period cause the length of injected rod before buckling to slowly decrease while smaller periods cause it to quickly decrease.

This project was motivated by the need to service wellbores in the oil industry. The oil industry requires a system that can: i) increase reach by 400% compared to the no rotation condition, ii) is able to be built on a large scale, and iii) is size and cost efficient. The data in figure 3.6 demonstrates that a system using on-off injection and continuous rotation at the injection site has the potential to increase reach by 400%. A continuous rotation system, however, is difficult to construct on a large scale. Another drawback is that on-off injection at a 50% duty cycle requires twice as long to reach the same distance as a constant injection system, thus increasing injection time.

Further work with on-off injection should examine the relaxation time for a rod being injected into a cylindrical constraint to change from a straight configuration to a helical configuration, while varying the length of rod in the cylinder. These values can help researchers understand how long the on-off injection can remain in the on-state before buckling at different lengths during injection. Combining the data with the data found in §3.1.1 and §3.1.2 can lead to an optimal duty cycle and period of on-off injection for various points inside the tube, thus leading to a time efficient method to increase the reach of the injected rod. Other parameters that can be explored with on-off injection include varying the clearance between the rod and the cylinder, varying the injection speed (amplitude of injection), varying the duty cycle, and exploring different periods with relation to §3.2. The results of this thesis should motivate further work in these directions.

Bibliography

- [1] E.K. Basset, A. H. Slocum, P. T. Masiakos, H. I. Pryor, O. C. Farokhzad,, and J. M. Karp. Design of a Mechanical Clutch-Based Needle-Insertion Device. *Proceedings of the National Academy of Sciences*, 106(14), pp. 5540-5545. 2009.
- [2] B. Bennetzen, J. Fuller, E. Isevcan, T. Krepp, R. Meehan, N. Mohammed, J. F. Poupeau, and K. Sonowal. Extended-Reach wells. *Oilfield Review*, 22(3), pp. 4-15. 2010
- [3] J. Cheatham, Jr. Helical Postbuckling Configuration of a Weightless Column Under the Action of Axial Load. *Journal of Petroleum Technology*, 24(4), pp. 467-472. 1984.
- [4] Y. Chen, Y. Lin, and J. Cheatham. Tubing and Casing Buckling in Horizontal Wells (Includes Associated Papers 21257 and 21308). *Journal of Petroleum Technology*, 42(2), pp. 140-141. 1990.
- [5] G. Deli, F. Liu, and B. Xu. An analysis of helical bucking of long tubulars in horizontal wells. *SPE International Oil and Gas Conference and Exhibition in China*. 1998.
- [6] B. Hughes. Rig count overview and summary count. November 2013.
- [7] A. Lubinski. A Study of the Buckling of Rotary Drilling Strings. *Drilling and Production Practice*, pp. 178-214. 1950.
- [8] I. McCourt, T. Trustlove, and J. Kubie. On the penetration of tubular drill pipes in horizontal oil wells. *Proceedings of the Institution of Mechanical Engineers, Part C: Journal of Mechanical Engineering Science*, 218(9), pp. 1063-1081. 2004.
- [9] J. Miller, Ph.D. Mechanical Behavior of Elastic Rods Under Constraint. *Massachusetts Institute of Technology*, pp. 45-223, 2014.
- [10] J. Miller, C. Mulcahy, J. Pabon, N. Wicks, and P. Reis. Extending the Reach of a Rod Injected Into a Cylinder Through Distributed Vibration. *Journal of Applied Mechanics*, 82. February 2015.
- [11] S. Miska and J. Cunha. An analysis of helical bucking of tubulars subjected to axial and torsional loading in inclined wellbores. *SPE Production Operations Symposium*. 1995.

- [12] R.F. Mitchell. Tubing Buckling – The State of the Art. *SPE Drill. Completion*, 23(4), pp. 361-370. 2008.
- [13] C. Mulcahy, J. Miller, T. Su, N. Wicks, J. Pabon, E.B. Dussan V, K. Bertoldi, and P. Reis. Rotation of a Seldner Rod Injected into a Cylindrical Constraint. *ASME 2014 International mechanical Engineering Congress & Exposition*. 2014.
- [14] P. Paslay and D. Bogy. The stability of a circular rod laterally constrained to be in contact with an inclined circular cylinder. *Journal of Applied Mechanics*, 31, pp. 605-610. 1964
- [15] L. Perneder and E. Detournay. Anomalous behaviors of a propagating borehole. *SPE Deepwater Drilling Completions Conference*. 2012.
- [16] T. Summers, H. A. Larsen, M. Redway, and G. Hill. The Use of Coiled Tubing During the Wytch Farm Extended Reach Drilling Project. *International Meeting on Petroleum Engineering*, pp. 23-36. 1995.
- [17] J. Wu and H. Juvkam-Wold. Study of helical bucking of pipes in horizontal wells. *SPE Production Operations Symposium*. 1993